SECOND EUROPEAN CONFERENCE ON EARTHQUAKE ENGINEERING
AND SEISMOLOGY, ISTANBUL AUG. 25-29, 2014

EXPERIMENTAL INVESTIGATION OF THE VISCID PROPERTIES OF LIQUEFIED SOIL UNDERGOING LARGE DEFORMATION

Salima Yasmine DRAIDI[1], Mounir NAILI[2] and Djillali BENOUAR[3]

ABSTRACT

This paper investigates the viscid properties of the liquefied soil undergoing large deformation as well as the behavior of adjacent soil around a model pile using a high speed CCD camera by means of a large dynamic geotechnical centrifuge. A new loading device was developed and connected to an embedded model pile able to sustain a centrifugal acceleration field of 50g and deliver a maximum stroke and velocity of 100 mm and 100 mm/s respectively. A trigger system was designed to operate and synchronize the actuator with the input ground motion, such as the developed lateral resistance can be monitored during all stage of liquefaction.

A series of dynamic centrifugal model tests were conducted by varying the relative density, the input ground motion, as well as the trigger time and the control direction of the actuator.

The viscid property of the liquefied soil is expressed by means of the apparent viscosity coefficient obtained through a back calculation using the formula proposed by Lamb, which expresses the drag force acting on a cylinder subjected to a flow of a viscous liquid. The derived values are within a comparable range to those derived for Jumoonjin sand for the same D_R using the dropping ball method but slightly higher than those estimated for Toyoura sand using different techniques as reported by J.I Hwang et al (2006).

INTRODUCTION

Liquefaction of loose, saturated, cohesionless soils and other granular materials represents one of the most devastating geotechnical hazards during large earthquakes. For instance, liquefaction induced ground failures have caused tremendous damage and disruption to pile foundations of buildings and bridges, embankments, river dikes, pipelines, lifelines system and waterfront structures (1964 Niigata, 1964 Alaska, 1971 San Fernando, 1983 Nihonkai Chubu, 1989 Loma Prieta, 1990 Luzon, 1995 Hyogoken- Nambu, 1999 Izmit, etc.).

Liquefaction-induced lateral spreading is known to occur on gently sloping ground or toward a steep open face such as river and river banks and results in relatively large displacements in the lateral direction. By reviewing and analyzing four case studies from past Japanese earthquakes namely the 1923 Kanto earthquake, Fukui earthquake of 1948, the 1964 Niigata earthquake and the 1983 Nihonkai-Chubu earthquake, Doi and Hamada (1992) investigated the mechanism of the occurrence of liquefaction induced ground displacements and its influence on underground structures. They showed that the resultant damage may extend over a region of hundreds square meters and the permanent

[1] Assistant Professor, Ecole Nationale Supérieure des Travaux Publics, Algiers, sy.draidi@yahoo.com
[2] Senior Researcher, Centre National de Recherche Appliquée en Génie Parasismique, Algiers, mounir.naili@gmail.com
[3] Professor, Faculty of Civil Engineering, Université des Sciences et de la Technologie Houari Boumedienne, Algiers, dbenouar@gmail.com

displacements may reach several meters even for mild ground slope. They stated that during Fukui earthquake, the maximum observed displacement in Morita area was greater than 4 m, and during Niigata earthquake, the maximum displacement reached 8 m in Ohgata area.

In order to protect these structures and to ensure their stability and serviceability during and after the earthquake shaking, the assessment of the likelihood induced permanent displacement and lateral spreading load is a matter of great concern in seismic proof design. Several models have been developed to predict the magnitude of the liquefaction induced ground displacements. They are based either on the empirical approach, simplified analytical methods or numerical approach. The latter relies on the absolute understanding of the nature of the liquefied soil to develop a comprehensive and consistent rheological model to represent the mechanism of the liquefaction and hence predict the magnitude of the induced displacement.

Although many studies were carried out to investigate the characteristics of the liquefied soil, the relationship between the stress and the strain which reaches sometimes 100 % is difficult to establish. The hypothesis of assuming the liquefied soil as an incompressible viscous fluid has been proposed and justified by many researchers. Moreover, Towhata et al. (1999) and many others showed that the apparent viscosity of the liquefied soil plays an important role in assessing the lateral resistance of the pile foundations, the induced lateral ground displacement, and the uplift displacement of underground structures as well as the subsidence of structures founded on liquefied ground. Several experimental studies attempted to assess the apparent viscosity of the liquefied soil using shaking table test, pulling-up and dropping ball methods and viscometer. The primary findings shows that the apparent viscosity increases by about 100 times (i.e. from 100~10000 Pa-s) for a relative density ranging from -30% to 50%.

In this study, a serie of dynamic centrifugal model tests was conducted in order to investigate the viscid properties of the liquefied soil undergoing large deformation as well as the behavior of adjacent soil around a model pile using a high speed CCD camera. Based on the tests results, a tentative proposal for suitable apparent viscosity value for liquefied soil are proposed to undertake numerical simulation to predict the magnitude of the lateral displacement due to liquefaction induced lateral spreading.

OVERVIEW OF THE POS-LIQUEFACTION SOIL BEHAVIOR

The nature characteristics of the liquefied soil have been investigated in the past decades with respects to post-earthquakes observations and physical modeling. In this respect, undrained triaxial compression tests, cyclic torsional shear tests and shaking table experiments have revealed that the liquefied soil behaves either as a solid or as viscous fluid or with combined characteristics during the course of the shaking as it was reported by Naili (2006).

. It was emphasized that the viscous liquid analogy is a useful concept in understanding the deformation of the liquefied soil deposit in lateral spread and the damage that occurred to many engineering facilities. However, this concept can not stand at the end of the shaking when the pore water pressure has totally dissipated and the subsoil has recovered part of its rigidity. It was concluded then, that the liquefied soil exhibits a dual behavior and a plausible explanation consists in assuming the liquefied soil as a viscous fluid during the course of the shaking, and as a solid with reduced rigidity after the dissipation of the pore water pressure.

Because the viscous fluid analogy is a useful concept, many researchers attempted to assess the apparent viscosity (or the viscosity coefficient) of the liquefied soil using various experimental testing. Shaking table experiment on model ground, laboratory shear test as well as viscometer, pile and steel ball pulling-up have been used to measure the viscosity of the liquefied soil. Tests results showed that the measured value lie in a range between 10 ~ 10000 Pa·s. Most importantly are the Hamada and Wakamatsu's test results that highlighted the non linear nature of the liquefied soil, by showing that the viscosity coefficient decreases with increasing shear strain rate. Using viscosity results obtained by viscometer, Uzuoka et al. derived a non linear relationship between the shear strain rate and the shear stress and proposed a Bingham type constitutive model for liquefied soil.

J.I Hwang et al.(2006) summarises and compares in Figure 1, the relationship between the equivalent Newtonian viscosity coefficient of liquefied soils behaving as viscous fluid and their relative density Dr, obtained by means of the different measurement techniques mentioned above.

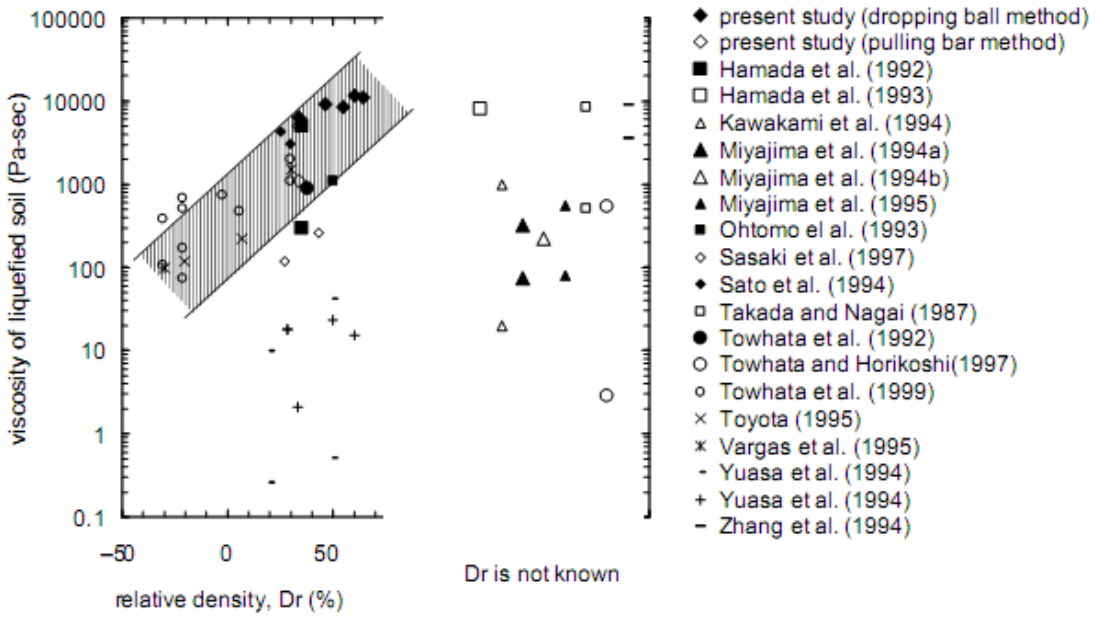

Figure 1. Relatioship between apparent viscosity of liquefied soils and relative density after J.I.Hwang (2006)

CENTRIFUGE MODEL TESTS

Methods of Experiments

In order to investigate the viscid properties of the liquefied soil, a new loading device as shown in Figure 2 was developed. This latter can be connected to an embedded model pile shown in Figure 3 able to sustain a centrifugal acceleration field of 50g and deliver a maximum stroke and velocity of 100 mm and 100 mm/s respectively. A trigger system was designed to operate and synchronize the actuator with the input ground motion, such as the developed lateral resistance can be monitored during all stage of liquefaction.

A series of dynamic centrifugal model tests were conducted by varying the relative density, the input ground motion, as well as the trigger time and the control direction of the actuator. The tests were conducted by means of the large dynamic geotechnical centrifuge located in the Public Works Research Institute, Japan with a radius of 6.6 m and a maximum payload of 40 ton-G (Matsuo et al., 1998).

A cross section of the instrumented actuator-pipe-model ground system is outlined in Figure 4 and the test conditions are summarized in Table 1. The models were prepared in a rigid steel container with inner dimensions of 80 cm long, 20 cm wide and 30 cm high. All models are prepared using Toyoura sand having a thickness of 24 cm. To fulfill the requirement in the similarity law, the sand layer was saturated by silicon oil having a viscosity of 50 centi-stokes.

In the tests, after applying a centrifuge acceleration of 50 G, a horizontal shaking was conducted. A sinusoidal wave of 20 cycles and 50 Hz was applied to case 1, 2, 5 and 6, while the ground motion recorded during the 1995 Hyogoken-Nanbu earthquake was applied to case 3 and 4.

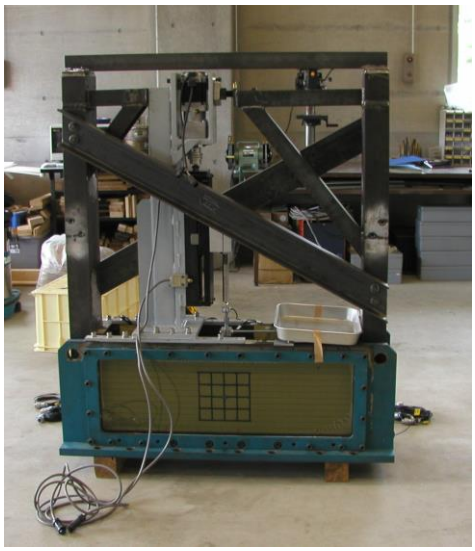

Figure 2. Designed loading device

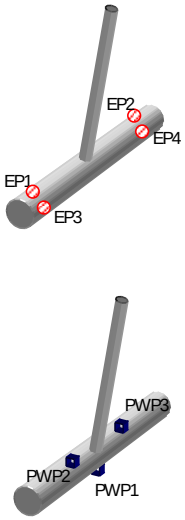

Figure 3. Embeded model pile

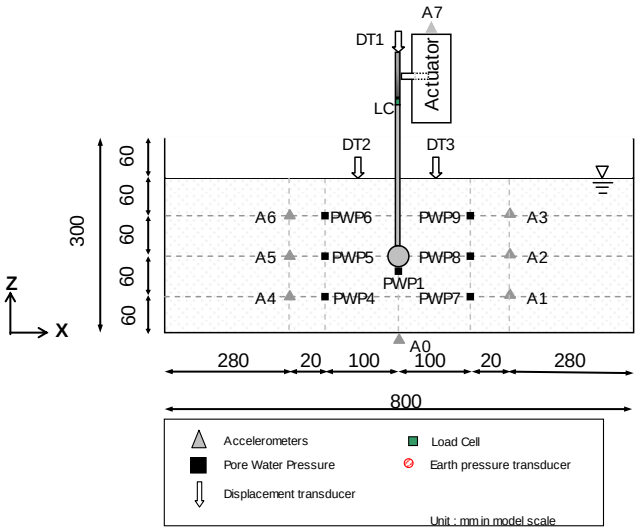

Figure 4. Centrifugal model configuration

Table 1. Test conditions

Experimental cases	Ground conditions				Centrifuge acceleration	Shaking conditions				Actuator control	
	Ground material	Dr (%)	Ground water level (mm)	N (g)	Wave type	Frequency (Hz)	Td (s)	A_0(g)	Disp rate (mm/s)		Trigger time
1	Toyoura sand	40	0	50	Sinusoidal	1	0.6	10	50	u	During
2		40					0.6			d	
3		50					0.6			u	After
4		50					0.6			d	
5		60			Kobe					d	During
6		60			Sinusoidal	1	0.6			u	

Ground deformation

Typical ground deformations that were taken before and after the test case 3 and 4 are presented in Figure 5 and Figure 6 respectively

Figure 5 (a). Ground model configuration before shaking for case 3

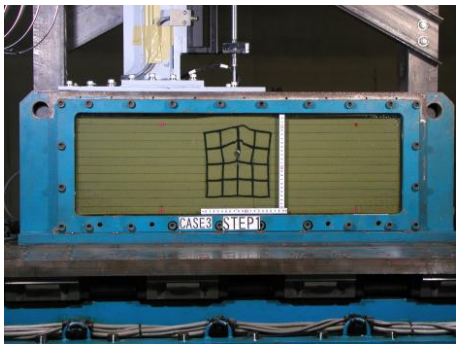

Figure 5 (b). Centrifugal model configuration after shaking for case 3

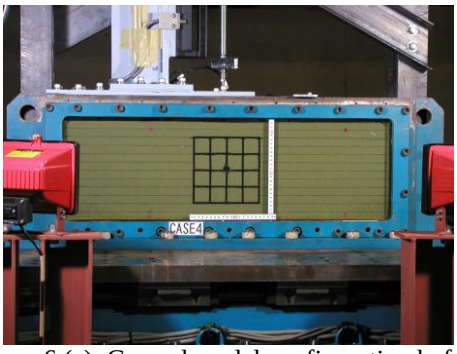

Figure 6 (a). Ground model configuration before shaking for case 4

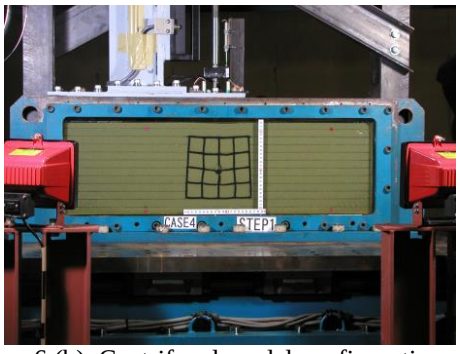

Figure 6 (b). Centrifugal model configuration after shaking for case 4

Test results

Typical results from Case 3 and Case 4 are outlined in what follow. Both experiments were conducted under similar conditions except for the sequence of the actuator control.

In test case 3, Figure 7 shows that the ground liquefies approximately 0.15 s after the start of the excitation, which corresponds to the first 3 or 4 cycles. The pile was pulled upward after the cease of the excitation. The drag force reached a maximum value of 5 kN while the pore water pressure reached a negative value at the level of the embedded pile.

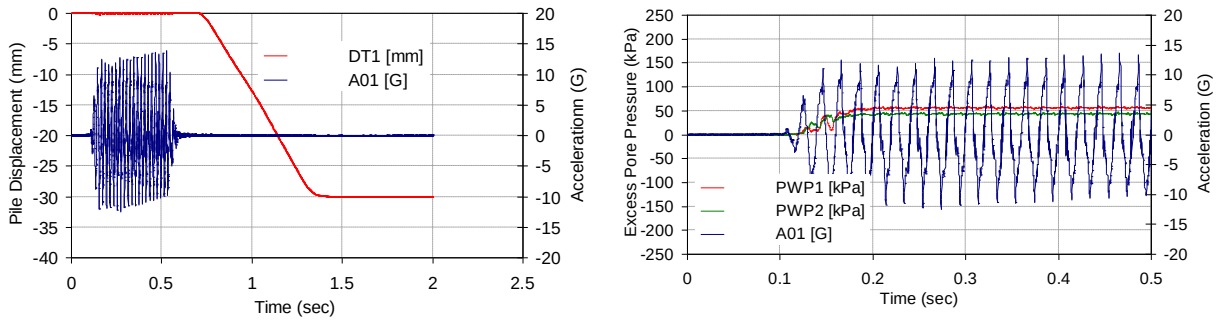

Figure 7. Relationship between excess pore pressure and pile displacement for test case 3

Figure 8 depicts the relationship between the excess pore water pressure at the level of the embedded pile PWP 1, PWP2, its vicinity PWP5, PWP6 and the resulting drag force. A maximum negative excess pore water pressure of 150 KPa is observed at the embedded pile when the drag force attains its maximum. This latter increased immediately as the drag force decreased when the pile achieves its maximum stroke at the value of 30 mm.

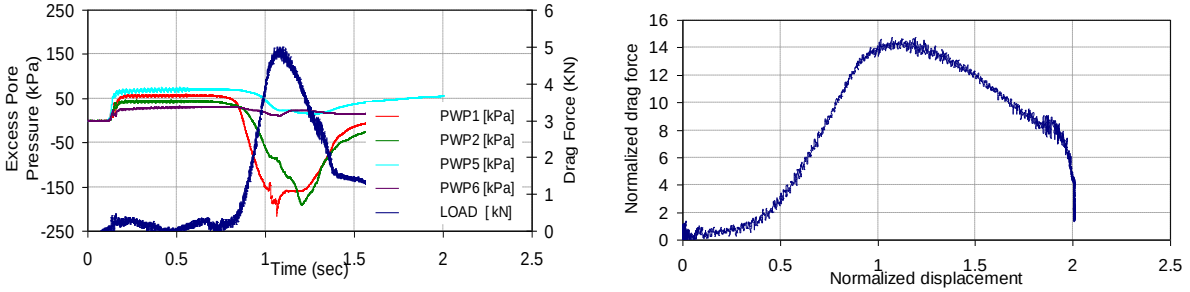

Figure 8. Relationship between excess pore pressure and drag force for test case 3

Similarly, Figure 9 and 10 represents respectively, the relationship between excess pore pressure at the pile level, its surrounding neighbourhood and the resulting drag force for test case 4.

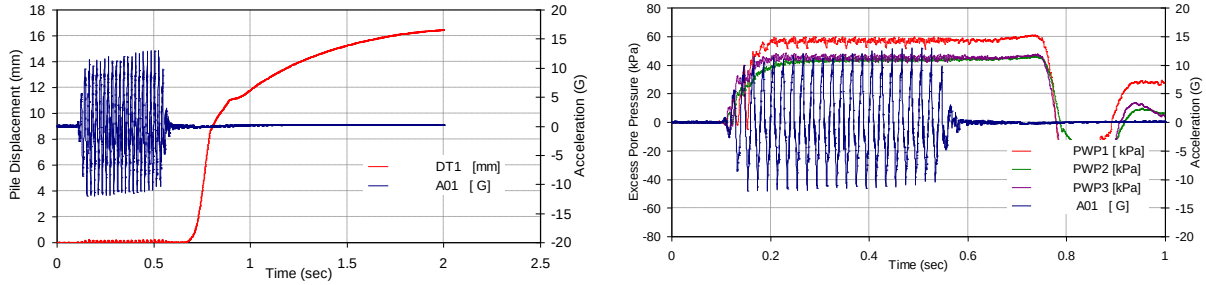

Figure 9. Relationship between excess pore pressure and pile displacement for test case 4

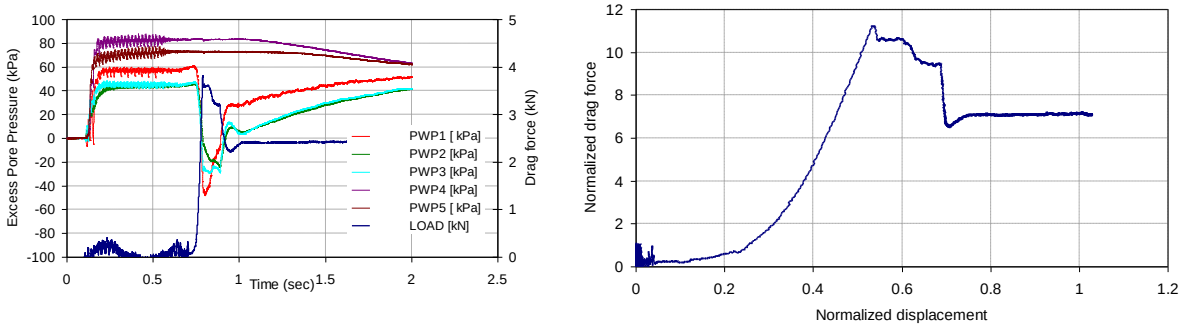

Figure 10. Relationship between excess pore pressure and drag force for test case 4

From the previous test results, the following observations can be made:

1. The excess pore pressure reached the maximum overburden initial effective stress during the first 3 cycles of the excitation. Whether the pile is pulled in the upward or in the downward direction, the movement induced a negative excess pore pressure at the top and the bottom of the pile. The drag force was fully mobilized when the negative excess pore pressure reached a minimum. In a quantitative manner, a value of 4 times the initial overburden effective stress was recorded in the upward direction while only 1 time of this value was recorded in the downward direction. The effect of the loading direction and the boundary conditions are clearly shown in this experiment.
2. The pore water pressure dissipation between the near field (adjacent to the pile) and the far field is different as illustrated in Figures (8) and Figure (10) respectively.
3. Figures (8) and (10) describe the relationship between the normalized drag force expressed by

$F^* = F/(\gamma HDLN)$ and the normalized displacement expressed by $U^* = U/D$. Where *F* is the measured drag force, γ the specific unit weight of the soil, *D* the pile diameter, *H* the initial embedded depth of the pile and *N* the centrifuge acceleration.

4. Though the values of the maximum normalized drag force are of comparable range in both cases, the mobilization distance is two times larger in the upward direction than in the downward direction.

Apparent soil viscosity determined from test results

An attempt to back calculate the apparent viscosity coefficient of the liquefied soil was undertaken using the formula proposed by Lamb, which expresses the drag force acting on a cylinder subjected to a flow of a viscous liquid.

$$F = 4\pi\eta VL/(2.002 - \ln(\rho VD/\eta)) \quad (1)$$

By substituting the measured value of the drag force into the previous expression, an apparent viscosity coefficient equals to η = 11600 Pa·s and 8200 Pa·s was estimated respectively for Case 3 and Case 4.

These values are within a comparable range to those derived for Jumoonjin sand for the same D_R using the dropping ball method but slightly higher than those estimated for Toyoura sand using different techniques as reported by J.I Hwang et al (2006).

CONCLUSIONS

During the past decades, several studies were carried out to investigate the characteristics of the liquefied soil as the relationship between the stress and the strain which reaches sometimes 100 % is difficult to establish. The hypothesis of assuming the liquefied soil as an incompressible viscous fluid has been proposed and justified by many researchers who showed that the apparent viscosity of the liquefied soil plays an important role in assessing the lateral resistance of the pile foundations, the induced lateral ground displacement, and the uplift displacement of underground structures as well as the subsidence of structures founded on liquefied ground.

This study investigates the viscid properties of the liquefied soil undergoing large deformation by means of a large geotechnical centrifuge located at the Public Works Research Institute. In this respect, a new loading device was developed and connected to an embedded model pile able to sustain a centrifugal acceleration field of 50g and deliver a maximum stroke and velocity of 100 mm and 100 mm/s respectively. A series of dynamic centrifugal model tests were conducted by varying the relative density, the input ground motion, as well as the trigger time and the control direction of the actuator.

The apparent viscosity coefficient of the liquefied soil is estimated using the formula proposed by Lamb, where an apparent viscosity coefficient equals to η = 11600 Pa·s and 8200 Pa·s was derived respectively for Case 3 and Case 4.

These values are within a comparable range to those derived for Jumoonjin sand for the same D_R using the dropping ball method but slightly higher than those estimated for Toyoura sand using different techniques as reported by J.I Hwang et al (2006).

It is worth mentioning that the results presented herein are only preliminary as the interpretation of test results from other experimental cases is underway. The final outcome of this study consists in proposing more reliable values for the apparent viscosity coefficient, so that the magnitude of the induced displacement due to liquefaction can be estimated with enough precision and the obtained values can be more consistent with the observed values during post-earthquake observations.

REFERENCES

The authors are grateful to the aid in grant from the Japan Society for the Promotion of Science who allowed conducting the experimental investigation using the large geotechnical centrifuge of the Public Works Research Institute, Japan during the postdoctoral research stay of the second author.

REFERENCES

Hwang J, Kim C, Chung C, Kim M. (2006) "Viscous fluid characteristics of liquefied soils and behavior of piles subjected to flow of liquefied soils", *Soil Dynamics and Earthquake Engineering* 26:313–23.

Lamb H. (1911) "On the uniform motion of a sphere through a viscous fluid". *Philosophical Magazine Journal of Science* S.6 (121):112–121.

Matsuo O, Tsutsumi T, Kondo K, Tamoto S (1998) "The dynamic geotechnical centrifuge at PWRI", *Proceedings of the International Conference on Centrifuge 98,* Tokyo, 25-30

Naili M (2006) Analysis of liquefaction induced ground displacement using Smoothed particle Hydrodynamics, Ph.D. Thesis, The University of Tsukuba, Japan

Towhata I, Vargas-Monge, W, Orense, R.P, Yao, M (1999) "Shaking table tests on subgrade reaction of pipe embedded in sandy liquefied subsoil", *Soil Dynamics and Earthquake Engineering,* 18, 347-361